Science Arts & Métiers (SAM)

is an open access repository that collects the work of Arts et Métiers ParisTech researchers and makes it freely available over the web where possible.

This is an author-deposited version published in: https://sam.ensam.eu
Handle ID: .http://hdl.handle.net/10985/8738

To cite this version :

Mathieu HOBON, Nafissa LAKBAKBI EL YAAQOUBI, Gabriel ABBA - Quasi Optimal Gait of a Biped Robot with a Rolling Knee Kinematic - In: 18th IFAC World Congress Milano (Italy) August 28 - September 2, 2011, Italy, 2011-08-28 - Preprints of the 18th IFAC World Congress Milano (Italy) August 28 - September 2, 2011 - 2011

Quasi Optimal Gait of a Biped Robot with a Rolling Knee Kinematic [⋆]

Mathieu Hobon [∗] **Nafissa Lakbakbi El Yaaqoubi** [∗∗]
Gabriel Abba [∗∗∗]

[∗] *Design, Manufacturing and Control Lab., Arts et Métiers ParisTech,*
57038 Metz Cedex 03, France (e-mail:
Mathieu.HOBON-8@etudiants.ensam.eu).
[∗∗] *National Engineering College of Metz, Technopôle, 57035 Metz*
Cedex, France (e-mail: lakbakbi@enim.fr)
[∗∗∗] *Design, Manufacturing and Control Lab., Arts et Métiers*
ParisTech, 57038 Metz Cedex 03, France (e-mail:
gabriel.abba@ensam.eu)

Abstract: In this paper, we address the problem of optimization of trajectories for a new class of biped robot. The knees of this biped are similar as the anthropomorphic one and have a rolling contact between the femur and the tibia. The robot has seven mechanical links and six actuators. The walking gait considered is a succession of single support phase (SSP) and impact of the mobile foot with the ground. Cubic uniform spline functions defined on a time interval express the gait for one step. An energy consumption function and a torques quadratic function are used to compare the new robot with anthropomorphic knees to a conventional robot with revolute joint knees. The minimization of the criteria is made with simplex algorithm. The physical constraints concerning the ZMP and the mobile foot behavior are respectively checked to make a step. Simulation results show that the energy consumption of the new biped with rolling knee contact is less than that of the robot with revolute joint knees.

Keywords: Biped design, energy optimization, parameter optimization, walking gait, cubic spline.

1. INTRODUCTION

The design of new mechanical architectures presents a major challenge in the coming years for the development and the use of biped robots or humanoids, see Chevallereau et al. (2009). In Sardain et al. (1998) and Sardain et al. (1999), the authors propose a structure of two linear actuators put in parallel, which control both degrees of freedom of ankle. A new architecture of the knee joint is proposed in Scarfogliero et al. (2004) for LARP robot. This innovative design presents a human-like knee with two rolling surfaces in contact. However, the authors do not consider a theoretical study to show the influence of this new design and there does not exist, our knowledge, an optimization of the walking for LARP robot, see Scarfogliero et al. (2005).

These new architectures of course require the development of control laws and larger adaptability of the tasks to be realized. Autonomy of decision but also energy autonomy contributes to these objectives. Therefore the determination of optimal trajectories of biped robots is a problem approached by the researchers since many years as in Cabodevila and Abba (1997). More recently, these studies concentrate on optimal trajectories of humanoid robots,

see Tlalolini (2008). These studies address three major issues:

- to improve, optimize or choose the kinematic structure of biped or humanoid robots,
- to define reference trajectories needed for the control methods, see Plestan et al. (2003),
- to determine the actuators or the mechanical drives as well as the whole of the elements of design and control.

The methods to determine optimal trajectories use several general ideas: trajectories resulting from a passive behavior of the robot, trajectories defined by a parametric formulation, trajectories inspired by the observation of biological systems (pattern generator design). Methods with passive trajectories can be discussed in McGeer (1990), Collins et al. (2001) and Wu and Yeh (2008). They are well adapted in the case of a specific robot structure used for the determination of passive trajectories, but are difficult to adapt to another structure or when to vary the mean velocity of the robot gait. The bio-inspired syntheses deal with the problem of the simultaneous design of the control and the synchronization of the movements of the legs. In this case, it is assumed that the robot is already designed and the objective is to find the control which optimizes the movement. This approach thus raises difficulties for optimization of mechanical architecture or for the choice of actuators. The third method based on seeking trajectories

while optimizing design or energy consumption criteria is better adapted to evaluate and validate a new kinematic structure. This method encounter difficulty due to the non linearity, the coupling of differential equation of the robot's behavior and do not present general solutions directly usable. The researchers thus very often propose one resolution by seeking a solution that is approached by projection in a set of orthogonal functions. The general problem is thus brought back to a parametric optimization, but requires to find in which set of functions one carries out projection. Several solutions were proposed these last years in Cabodevila (1997) and in Chevallereau and Aoustin (2001). The search for a stable cyclic walk with fixed speed led the researchers to define the trajectory coordinates using truncated Fourier series, see Cabodevila (1997) and Shafii et al. (2010). Polynomial or cubic spline functions were also often used, see Roussel et al. (1998), Tlalolini et al. (2009) and Banno et al. (2009).

The resolution of the parametric problem of optimization is not obvious and led to several very interesting developments. When one seeks walking gait for a robot with n-DOF projected in a set of p orthogonal functions, one seeks finally $n \times p$ parameters. Moreover, constraints on the mobile foot trajectory, contact and nonslip of the fixed foot on the ground and limitations of the actuator torques are expressed with nonlinear functions in the space of the parameters. Thus, several authors propose to use powerful algorithms of optimization to solve the problem. Among them, the mostly used is the real-coded genetic algorithm as in Park and Choi (2004).The parameters are gathered in chromosomes and genes and a set of individuals is generated randomly. Then, the algorithm find the best individual which minimizes a given criterion. For 3D humanoid robots, the n number of DOF increases and certain authors also propose swarm optimization techniques, see Shafii et al. (2010) or simulated annealing techniques, see Hajek (1988). If there are few $n \times p$ of parameters , it is possible to use simpler algorithms like simplex or gradient techniques, see Fletcher (1987).

In this work, the trajectories are expressed with cubic uniform spline functions. Section 2 explains the geometric and dynamic models of the two robot architectures considered. Section 3 defines the procedure for obtaining the joint coordinate function, the constraints of smoothness, cyclicity and the vector of parameters to optimize. Section 4 presents the optimization problem, candidate criteria used to optimize the walking gait and the constraints linked to the achievement of the trajectory with impact. Finally, results of simulations and optimizations are presented in Section 5.

2. BIPED MODELING

This work focuses on a planar biped robot with seven mechanical links including a trunk, two thighs, two legs and two feet. The articulations are all revolute joints and fully actuated. The articulations are placed at the hips, the knees and the ankles. A second robot kinematic structure is similar to the first except the knees where the revolute joint is replaced by a joint of two rolling contact surfaces between the thigh and the leg, see Scarfogliero et al. (2004). Figures 1 and 2 represent the two robot

structures by defining the reference frame and the associated variables. The angular coordinates $q_i, \{i = 1 \cdots 7\}$ of orientation of each body are with references to vertical coordinate. The parameters of the model are the lengths l_i of each body C_i, the masses m_i, the position s_i of the centers of mass Cg_i and the moments of inertia I_i of each body around the axis y_0 go through Cg_i. The moment of inertia of the actuators and of the elements of transmission was included with the moment of inertia I_i. The foot geometry is defined by the length of the foot sole $T_1 H_1 = L_p$, the distance $O_0 H_1 = l_p$ and the altitude of the ankle $O_0 A_1 = h_p$. For the robot with rolling knee contact, figure 3 gives the detail of the knee articulation by supposing that the two bodies in contact roll without slip and end in a cylindrical surface of radius r_1 for the leg and radius r_2 for the thigh. In order to compare the two robots of identical global height, lengths between the center of the ankle (resp. hips) are decreased by the values r_1 (resp. r_2). The geometrical model of the second structure of robot is then given by the following equations:

- position of the hip center

$$x_H = -l_1 \sin q_1 - l_2 \sin q_2 \qquad (1)$$
$$z_H = l_1 \cos q_1 + l_2 \cos q_2 + h_p \qquad (2)$$

- position of the heel of the mobile foot

$$x_{H_2} = x_H + l_1 \sin q_4 + l_2 \sin q_3$$
$$\qquad -l_p \cos q_{p2} + h_p \sin q_{p2} \qquad (3)$$
$$z_{H_2} = z_H - l_1 \cos q_4 - l_2 \cos q_3$$
$$\qquad -l_p \sin q_{p2} - h_p \cos q_{p2} + h_p \qquad (4)$$

- position of the toes of the mobile foot

$$x_{T_2} = x_H + l_1 \sin q_4 + l_2 \sin q_3$$
$$\qquad - (l_p - L_p) \cos q_{p2} + h_p \sin q_{p2} \qquad (5)$$
$$z_{T_2} = z_H - l_1 \cos q_4 - l_2 \cos q_3$$
$$\qquad - (l_p - L_p) \sin q_{p2} - h_p \cos q_{p2} + h_p \qquad (6)$$

For the second kinematics with the rolling knee contact, a geometric model with additional terms is obtained. As shown in the figure 3, the position between the thigh and the leg depend on the distance $l = r_1 + r_2$ and of the angle γ_1 for the fixed leg (resp. γ_2 for the mobile leg) defined by the angle to vertical of the segment connecting the two centers C_1 and C_2 of the left knee (resp. right knee). To keep total height of the two robot identical, the lengths of the thighs and legs l_1 and l_2 are replaced by the distances $C_1 A_1 = l'_1 = l_1 - r_1$ and $C_2 H_1 = l'_2 = l_2 - r_2$. The coordinates of the hip, the heel and the toe of the mobile foot of the new structure are (x'_H, z'_H), (x'_{H_2}, z'_{H_2}) and (x'_{T_2}, z'_{T_2}) respectively.

- position of the hip center

$$x'_H = -l'_2 \sin q_2 - l \sin \gamma_1 - l'_1 \sin q_1 \qquad (7)$$
$$z'_H = l'_2 \cos q_2 + l \cos \gamma_1 + l'_1 \cos q_1 + h_p \qquad (8)$$

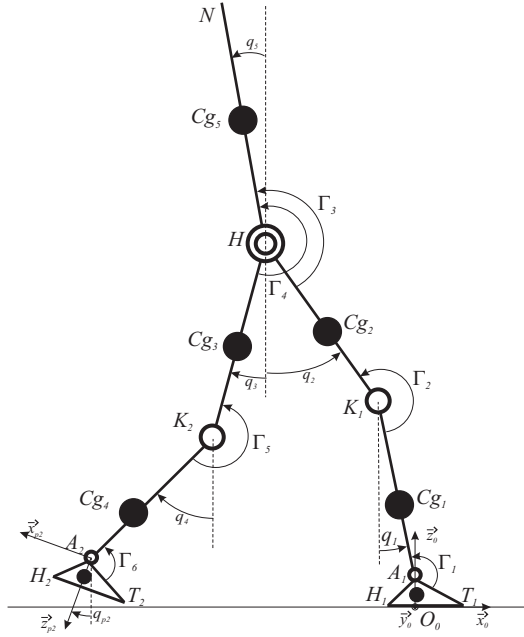- position of the heel of the mobile foot

Fig. 1. *Definition of reference frame, coordinates, centers of gravity and mass of standard robot*
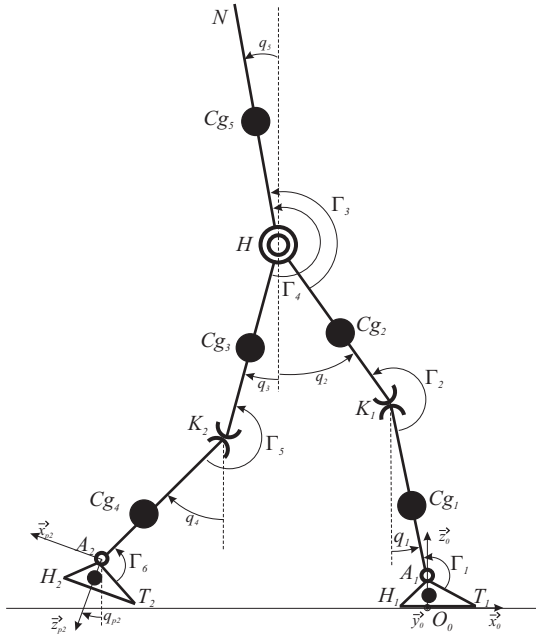

Fig. 2. *Definition of reference frame, coordinates, centers of gravity and mass of rolling knee robot*

$$x'_{H_2} = x'_H + l'_2 \sin q_3 + l \sin \gamma_2 + l'_1 \sin q_4$$
$$- l_p \cos(q_{p2}) + h_p \sin(q_{p2}) \qquad (9)$$

$$z'_{H_2} = z'_H - l'_2 \cos q_3 - l \cos \gamma_2 - l'_1 \cos q_4$$
$$- l_p \sin(q_{p2}) - h_p \cos(q_{p2}) + h_p \qquad (10)$$

- position of the toes of the mobile foot

$$x'_{T_2} = x'_H + l'_2 \sin q_3 + l \sin \gamma_2 + l'_1 \sin q_4$$
$$- (l_p - L_p) \cos(q_{p2}) + h_p \sin(q_{p2}) \qquad (11)$$

$$z'_{T_2} = z'_H - l'_2 \cos q_3 - l \cos \gamma_2 - l'_1 \cos q_4$$
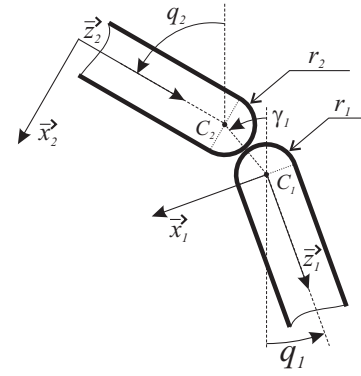$$- (l_p - L_p) \sin(q_{p2}) - h_p \cos(q_{p2}) + h_p \qquad (12)$$

Fig. 3. *Detailed design of the rolling knee solution*

with $\gamma_1 = \frac{r_1 \, q_1 + r_2 \, q_2}{l}$ and $\gamma_2 = \frac{r_1 \, q_4 + r_2 \, q_3}{l}$.

For small angles q_1 and q_2, the angle γ_1 is also small and $x_H - x'_H \cong 0$ as $z_H - z'_H \cong 0$. The difference between the two kinematic structures is thus more important when the angle between the two legs increases.

In order to synthesize the trajectories, walking phases are initially described. The study is limited to a gait composed of a succession of simple support phase (SSP) followed by an impact between the mobile foot and the ground. It is assumed thereafter that during the simple support phase, the left foot is always in contact with the ground. The articular angle of the left foot q_{p1} is thus always zero. The contact of the left foot results in a holonomic constraint for the rolling knee robot defined by the equations:

$$z'_{H_1} = 0 \qquad (13)$$
$$q_{p1} = 0 \qquad (14)$$

Moreover, it is supposed that the foot in contact does not slip, which represents a nonholonomic constraint for the robot.

$$x'_{H_1} - l_p = 0 \qquad (15)$$

Differentiating twice the equations (13) to (15) of holonomic and nonholonomic constraints yields:

$$A_c(q)\ddot{q} + H_c(\dot{q}, q) = 0 \qquad (16)$$

The matrix $A_c \in \mathbb{R}^{3\times 9}$ is given by the following expression:

$$A_c = \begin{bmatrix} 0 & 0 & \begin{matrix} r_1 \cos \gamma_1 + \\ l'_1 \cos q_1 \end{matrix} & \begin{matrix} r_2 \cos \gamma_1 + \\ l'_2 \cos q_2 \end{matrix} & 0 & 0 & 0 & 1 & 0 \\ 1 & 0 & 0 & 0 & 0 & 0 & 0 & 0 & 0 \\ 0 & 0 & \begin{matrix} r_1 \sin \gamma_1 + \\ l'_1 \sin q_1 \end{matrix} & \begin{matrix} r_2 \sin \gamma_1 + \\ l'_2 \sin q_2 \end{matrix} & 0 & 0 & 0 & 0 & 1 \end{bmatrix} \qquad (17)$$

The vector $H_c \in \mathbb{R}^{3\times 1}$ is defined by:

$$H_c(\dot{q}, q) = \qquad (18)$$

$$\begin{bmatrix} -\left(\dfrac{r_1{}^2}{l} \sin \gamma_1 + l'_1 \sin q_1\right) \dot{q}_1^2 - \dfrac{2 r_1 \, r_2}{l} \sin \gamma_1 \, \dot{q}_1 \, \dot{q}_2 \\ \quad - \left(l'_2 \sin q_2 + \dfrac{r_2{}^2}{l} \sin \gamma_1\right) \dot{q}_2^2 \\[2ex] 0 \\[2ex] \left(\dfrac{r_1{}^2}{l} \cos \gamma_1 + l'_1 \cos q_1\right) \dot{q}_1^2 + \dfrac{2 r_1 \, r_2}{l} \cos \gamma_1 \, \dot{q}_1 \, \dot{q}_2 \\ \quad + \left(l'_2 \cos q_2 + \dfrac{r_2{}^2}{l} \cos \gamma_1\right) \dot{q}_2^2 \end{bmatrix}$$

The method of determination of the robot dynamic model during SSP is largely known, see Spong and Vidyasagar (1991) and Khalil and Dombre (2002). The vector of the generalized coordinates contains the revolute joint articular angles of the seven links of the robot and the Cartesian coordinates of the center of the hips. From the Lagrange equations, the following equation is obtained:

$$D(q)\ddot{q} + H(\dot{q},q) + Q(q) = B\Gamma + A_c^{\mathrm{T}}(q)F_e \qquad (19)$$

with $q = [q_{p1}\ q_{p2}\ q_1\ q_2\ q_3\ q_4\ q_5\ x_H\ z_H]^{\mathrm{T}}$ the absolute coordinate vector, $\dot{q} = [\dot{q}_{p1}\ \dot{q}_{p2}\ \dot{q}_1\ \dot{q}_2\ \dot{q}_3\ \dot{q}_4\ \dot{q}_5\ \dot{x}_H\ \dot{z}_H]^{\mathrm{T}}$ the absolute velocity vector, $D(q) \in \mathbb{R}^{9\times 9}$ the mass-inertia matrix, $H(\dot{q},q)$ summarizes vector of centrifugal and Coriolis effects, Γ the articular torques vector (the direction of application of the torques is indicated on figure 1), B the control matrix, $Q(q)$ summarizes the forces and torques vector due to gravity and $F_e = [F_x\ F_z\ C_y]^{\mathrm{T}}$ the ground wrench (external forces and torque) which are exerted on the foot in support.

The expression of the torque vector is relatively simple since there are six motors on the hips, knees and ankles articulations, from where $\Gamma = [\Gamma_1\ \Gamma_2\ \Gamma_3\ \Gamma_4\ \Gamma_5\ \Gamma_6]^{\mathrm{T}}$.
The control matrix B is given by:

$$B = \begin{bmatrix} -1 & 0 & 0 & 0 & 0 & 0 \\ 0 & 0 & 0 & 0 & 0 & -1 \\ 1 & -1 & 0 & 0 & 0 & 0 \\ 0 & 1 & -1 & 0 & 0 & 0 \\ 0 & 0 & 0 & -1 & 1 & 0 \\ 0 & 0 & 0 & 0 & -1 & 1 \\ 0 & 0 & 1 & 1 & 0 & 0 \\ 0 & 0 & 0 & 0 & 0 & 0 \\ 0 & 0 & 0 & 0 & 0 & 0 \end{bmatrix} \qquad (20)$$

The second robot configuration (see fig.2) differs from the standard configuration (see fig.1) by additional terms in the matrices of the dynamic model. The forms of the matrices $D(q)$ and $A_c(q)$ and of the vector $Q(q)$ of the dynamic model for the structure of robot with rolling knees are given in appendix A.

The vector $H(\dot{q},q)$ is not given because it can be deduced simply from $D(q)$ using the Christoffel symbols. The complete study of walk requires the modeling of the phases of impact which occur before and after each phase of simple support. Before impact and at the beginning of phase of simple support, it is assumed that the right foot is on the ground while the left foot impacts. The equations of impact are then obtained by:

$$D(q)\left(\dot{q}^+ - \dot{q}^-\right) = A_c^T I_R \qquad (21)$$

$$A_c(q)\ \dot{q}^+ = 0 \qquad (22)$$

with $A_c(q)$ defined by (19), $\dot{q}^- = \dot{q}(0^-)$ and $\dot{q}^+ = \dot{q}(0^+)$. The resolution of this system of equations gives the following results:

$$\dot{q}^+ = \left[I_9 - D^{-1}A_c^T(A_c D^{-1} A_c^T)^{-1} A_c\right]\dot{q}^- \qquad (23)$$

$$I_R = (A_c D^{-1} A_c^T)^{-1} A_c \dot{q}^- \qquad (24)$$

By finding the speed vector after impact what enables us to initialize the trajectories defined in the following section.

3. EXPRESSION OF THE GAIT PARAMETRIC TRAJECTORY

3.1 Cubic spline angular coordinates

In this work, the articular angles are defined by cubic uniform spline functions. In order to simplify the expression of the spline function, the time t is normalized to the dimensionless time variable $t_n = t/T$ where T is the period of one step. The knot vector t_k for the spline has three knots given by $t_k = [\,0\ 0.5\ 1\,]$. In the neighborhood of $t_i \in t_k, i \in [0,1,2]$, the spline function has smoothness $\mathcal{C}^1$. In fact, it is presume that the second derivative of the spline function is not necessarily continuous at $t_1 = 0.5$, but the optimization process can lead to a choice of parameters which returns the function to be continued at this knot. In the neighborhood of $t_0 = 0$ and $t_2 = 1$, the spline is inevitably $\mathcal{C}^1$ while the impact model imposes a discontinuity of the speed at this moment. At the beginning of the step ($t_n = 0$), we suppose that the mobile leg has a x-coordinate behind of that of the trunk. At the end of the step ($t_n = 1$), the mobile leg has advanced of a distance d and is in front of the trunk.

The general form of the spline function for the angular coordinates is also given by:

$$0 \le t_n \le \tfrac{1}{2} \rightarrow f_{q_i}(t_n) = a_0 + a_1 t_n + a_2 t_n^2 + a_3 t_n^3 \qquad (25)$$

$$\tfrac{1}{2} \le t_n \le 1 \rightarrow \begin{aligned} f'_{q_i}(t_n) = {}& b_0 + b_1(1-t_n) + b_2(1-t_n)^2 \\ & + b_3(1-t_n)^3 \end{aligned} \qquad (26)$$

with $q_i \in [q_{p2}, q_1, q_2, q_3, q_4, q_5]$ the angular coordinates, a_j and b_j, $j = [0 \cdots 3]$ the eight parameters are necessary to express each angular coordinates. The corresponding speed and acceleration are obtained by derivation of the preceding expressions.

3.2 Smoothness, cyclicity and ground boundary conditions

During the SSP, the left foot (fixed foot) is supposed to be in contact with the ground without slip or rebound and his position is horizontal, also $q_{p1}(t) = 0$. The (x_H, z_H)-coordinates of the hip can also be deduced from the expression of the angular coordinates by using the equation (1) or (7). The six other angles $[q_{p2}, q_1, q_2, q_3, q_4, q_5]$ from the coordinate vector are defined by a general spline function given by equations (25) and (26). We also need at most 24 parameters but smoothness and cyclicity conditions will reduce this number. The hypotheses are:

- considering that the mobile foot is flat on the ground at the start and end of each step,
- the speed of the mobile foot is null of the end of step,
- the angles of trunk and of the mobile foot are T-periodic,
- the thigh and leg angles are $2T$-periodic.

Smoothness and cyclicity conditions lead to:

- for the mobile foot angle: $f_{q_{p2}}(0) = f'_{q_{p2}}(1) = 0$, $f_{q_{p2}}(0.5) = f'_{q_{p2}}(0.5)$,
- for the trunk angle: $f_{q_5}(0) = f'_{q_5}(1)$, $f_{q_5}(0.5) = f'_{q_5}(0.5)$,
- for the thigh angles: $f_{q_2}(0) = f'_{q_3}(1)$, $f_{q_3}(0) = f'_{q_2}(1)$, $f_{q_2}(0.5) = f'_{q_2}(0.5)$, $f_{q_3}(0.5) = f'_{q_3}(0.5)$,

- for the leg angles: $f_{q_1}(0) = f'_{q_4}(1)$, $f_{q_4}(0) = f'_{q_1}(1)$, $f_{q_1}(0.5) = f'_{q_1}(0.5)$, $f_{q_4}(0.5) = f'_{q_4}(0.5)$,

- for the mobile foot speed: $\dot{f}'_{q_{p2}}(1) = 0$, $\dot{f}_{q_{p2}}(0.5) = \dot{f}'_{q_{p2}}(0.5)$,

- for the trunk speed: $\dot{f}_{q_5}(0.5) = \dot{f}'_{q_5}(0.5)$,

- for the thigh speeds: $\dot{f}_{q_2}(0.5) = \dot{f}'_{q_2}(0.5)$, $\dot{f}_{q_3}(0.5) = \dot{f}'_{q_3}(0.5)$,

- for the leg speeds: $\dot{f}_{q_1}(0.5) = \dot{f}'_{q_1}(0.5)$, $\dot{f}_{q_4}(0.5) = \dot{f}'_{q_4}(0.5)$.

The impact conditions impose:

- for the mobile foot: $\dot{f}_{q_{p2}}(0) = \dot{f}'_{q_{p2}}(1) + \Delta_1$

- for the trunk: $\dot{f}_{q_5}(0) = \dot{f}'_{q_5}(1) + \Delta_6$

- for the thighs: $\dot{f}_{q_2}(0) = \dot{f}'_{q_3}(1) + \Delta_3$; $\dot{f}_{q_3}(0) = \dot{f}'_{q_2}(1) + \Delta_4$

- for the legs: $\dot{f}_{q_1}(0) = \dot{f}'_{q_4}(1) + \Delta_2$; $\dot{f}_{q_4}(0) = \dot{f}'_{q_1}(1) + \Delta_5$

with $\Delta_i, i \in [1 \cdots 6]$ are calculated by the impact model (23) and detailed in appendix B.

Considering the preceding conditions, one needs 22 parameters to describe the trajectories. Furthermore, it is more practical to use the inverse geometric model to obtain the initial angular positions. Also the values $[f_{q_1}(0), f_{q_2}(0), f_{q_3}(0), f_{q_4}(0)]$ are deduced from the Cartesian positions of the hip $(x_H(0), z_H(0))$. Additionally, the variable T is put in the parameter vector. Finally $p = \left[x_H(0), z_H(0), f_{q_5}(0), \dot{f}'_{q_i}(1), \ddot{f}_{q_i}(0), \ddot{f}'_{q_i}(1), T \right]$, the parameter vector contains 21 parameters and is used for the optimization process. A simple linear system gives us the relation between p and (a_j, b_j) of (25) and (26).

4. OPTIMIZATION PROBLEM

From models and trajectories developed in the preceding sections, the optimization problem is defined as to find a solution minimizing a performance criterion based on the parameter vector of the gait. The problem is solved by fixing parameters to define the articular angle evolution and determine the criterion within the constraints imposed by physics. The unilateral foot contact on the ground imposes a positive force reaction F_z. The ZMP position must stay inside surface of the foot support. Constraints of the foot moving above the ground are obtained through the Cartesian positions of the swing leg. The choice was made considering that knees can not bend backward and adding therefore two noninverting constraints of the knees. These constraints are handled in the minimization process with Lagrange multipliers penalty method. The optimization problem reduces to:

$$\min_p C(p) \qquad (27)$$

under $\Psi(p) \geq 0$

$$\Psi(p) = [\Psi_1 \Psi_2 \Psi_3 \Psi_4 \Psi_5 \Psi_6 \Psi_7]^{\mathrm{T}} \qquad (28)$$

with $\Psi_1 = F_z$, $\Psi_2 = x_{ZMP} + l_p$, $\Psi_3 = -x_{ZMP} + (L_p - l_p)$, $\Psi_4 = q_2 - q_1$, $\Psi_5 = q_3 - q_4$ and according to the standard robot respectively the rolling knee robot $\Psi_6 = z_{H_2}$ (resp. $\Psi_6 = z'_{H_2}$) and $\Psi_7 = z_{T_2}$ (resp. $\Psi_7 = z'_{T_2}$) manage that the swing leg does not touch the ground during the single support.

The ground reaction forces are obtained through the dynamic model with the generalized coordinates.

The x-coordinate of the ZMP is defined by:

$$x_{ZMP} = \frac{\Gamma_1 - h_p F_x}{F_z} \qquad (29)$$

Many optimization methods are related by Fletcher (1987) or by Hajek (1988). The choice was made using the method of Nelder-Mead simplex like optimization algorithm. The simplex method is based on the construction of a polytope with $N+1$ vertices in N-dimensional space. This involves finding the closest vertex to the optimal solution and performs the pivoting rules for finding the minimum. All the constraints are added in the criterion with the function given in (30) and this problem is so transformed in an unconstrained problem. The Nelder-Mead simplex algorithm can also solve it (see Lagarias et al. (1998)). With this type of algorithm, it avoids local minima more easily. It can boost the final value of the parameters obtained to see if the optimal minimum is well found.

In the literature, many optimization criteria are used, e.g. torque quadratic criterion in Tlalolini et al. (2009) or mechanical energy criterion in Scheint et al. (2008). In our study, we focused on two features. The first function used is a sthenic function, i.e. torque quadratic function that allows to determine the Joule loss in the actuators during a walking step. This function is expressed as:

$$C_\Gamma = \frac{2}{d} \int_0^T \left(\Gamma^{\mathrm{T}} \Gamma + k \sum_{i=1}^7 (e^{(|\Psi_i| - \Psi_i)} - 1) \right) d\tau + Err \quad (30)$$

with Γ is determined from the dynamic model (19).

Note that in (30), we add penalty functions expressed by $k(e^{(|\Psi_i| - \Psi_i)} - 1)$. Each constraint is represented by a penalty function where Ψ_i is replaced by (28). The weighting factor k is arbitrarily chosen to 10^6. Err can handle errors during the determination of the inverse geometric model. At the end of optimization, all penalty functions and Err are in all cases equal to zero.

The second function define the mechanical energy consumption (31). Because the actuators are not reversible, the function is obtained by the sum of the absolute values of mechanical energy of each joint. The constraints are also handled by penalty method.

$$C_E = \int_0^T \left(\sum_{i=1}^6 |\Gamma_i \dot{\theta}_i| + k \sum_{i=1}^7 (e^{(|\Psi_i| - \Psi_i)} - 1) \right) d\tau + Err \qquad (31)$$

$\dot{\theta}$ represents the vector of the relative velocities of each joint and is defined in (32).

$$\dot{\theta} = \begin{bmatrix} \dot{\theta}_1 \\ \dot{\theta}_2 \\ \dot{\theta}_3 \\ \dot{\theta}_4 \\ \dot{\theta}_5 \\ \dot{\theta}_6 \end{bmatrix} = \begin{bmatrix} \dot{q}_1 - \dot{q}_{p1} \\ \dot{q}_2 - \dot{q}_1 \\ \dot{q}_5 - \dot{q}_2 \\ \dot{q}_5 - \dot{q}_3 \\ \dot{q}_3 - \dot{q}_4 \\ \dot{q}_4 - \dot{q}_{p2} \end{bmatrix} \qquad (32)$$

5. SIMULATION AND RESULTS

The robot studied is with anthropomorphic data. It height is 1.70 m for a total mass of 70 kg. The following table

summarizes the parameters of each body. The radii r_1 et r_2 have been set at 0.05 m.

Table 1. Robot data

Bodies	Lengths [m]	Masses [kg]	Inertia moments [kg.m^2]	Positions of CoM [m]
Feet	$L_p = 0.2584$ $l_p = 0.0935$ $h_p = 0.0663$	1.015	0.001	0.0331
Leg	0.4182	3.2550	0.0519	0.1811
Thigh	0.4165	7.00	0.1267	0.1803
Trunk	0.7990	47.46	7.4539	0.5002

In the first part, we will perform an optimization with sthenic criterion for the standard robot (ck) and the rolling knee robot (rk). We will compare the sthenic criterion depending on forward speed for both robots. We look at energy function that is performed without optimization. We will observe the evolution of torques, angles and the ground reaction forces for the optimal walking speed. In a second step, we will optimize the second criterion for energy as a function of walking speed and then we will look the sthenic function. We can see on figure 4 that

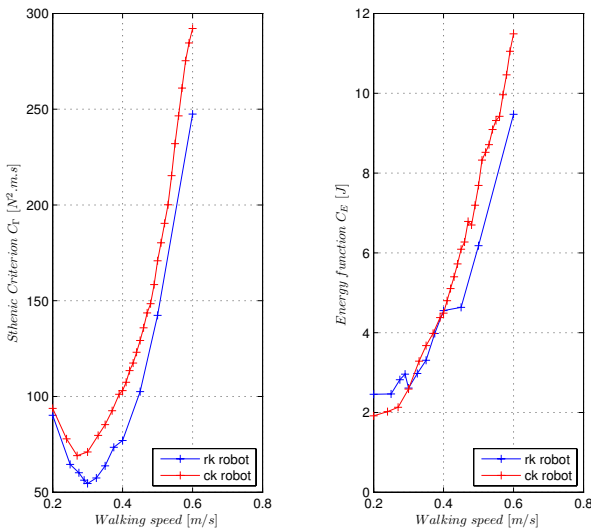Fig. 5. Comparison of torques for the walking speed to 0.3 m/s

Fig. 4. Evolution of optimal sthenic criterion versus walking speed (on the left). Evolution of the corresponding energy function (on the right).

the sthenic criterion for the rolling knee robot is lower to the same criterion for the standard robot. There was a reduction of about 17 %. The speed corresponding to the minimal value of the criterion is respectively 0.27 m/s for the standard robot and 0.3 m/s for the rolling knee robot.

The figure 5 shows that the torques of both structures have similar shapes. The torque Γ_2 of the supporting knee is more important at the initial time for the structure "rk" and lower at the step end. Unlike for the "ck" structure, the torque Γ_2 is lower initially and higher at the end of step. The angles are represent on (figure 6). We note that the angle q_4, corresponding to the swinging leg, bent more quickly on the "rk" robot than on the standard structure. It allows the supporting leg staying right in the case of
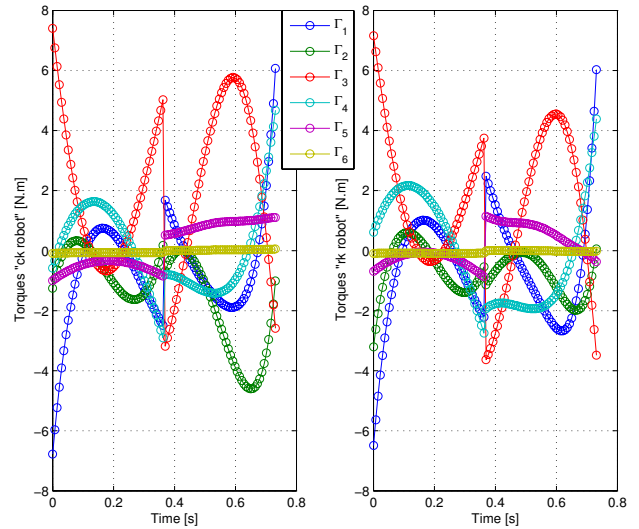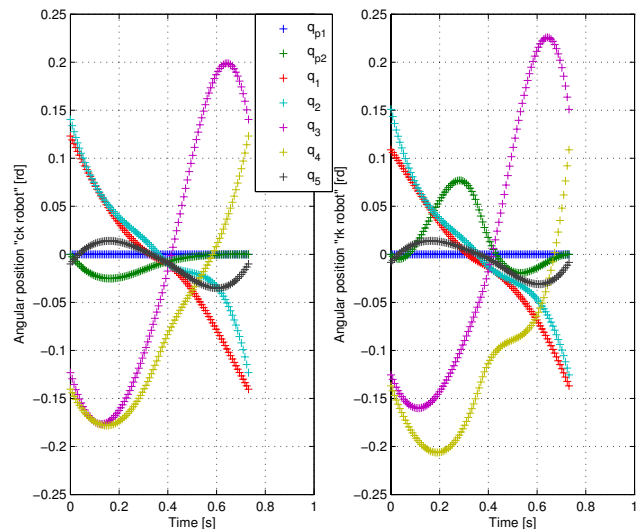

Fig. 6. Comparison of angles for the walking speed to 0.3 m/s

the "rk" robot while the supporting leg of "ck" robot bends toward at the end of the step. Figure 7 gives us a tangential to normal force ratio lower than usual Coulomb friction coefficient and confirms that the robot does not slide during the movement phase. In figure 8, we show that the rolling knee structure uses less energy than standard robot structure. We also note that the sthenic function is much more sensitive than the energy criterion.

6. CONCLUSION

The optimization process gives us an energetic gain of about 11 % for the rolling knee robot. In our ANR program [1], this approach will be applied to the robot
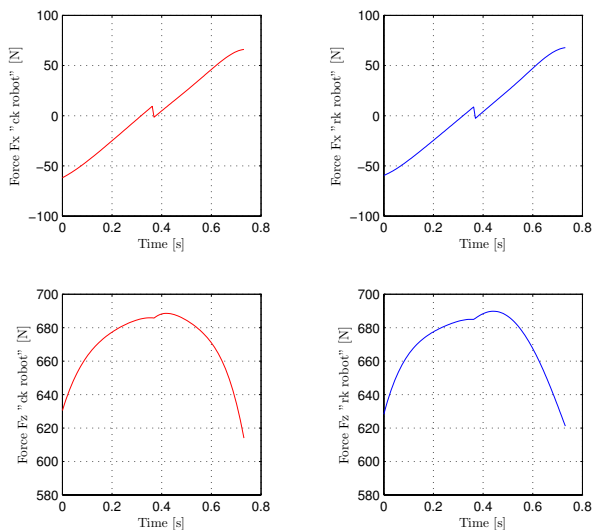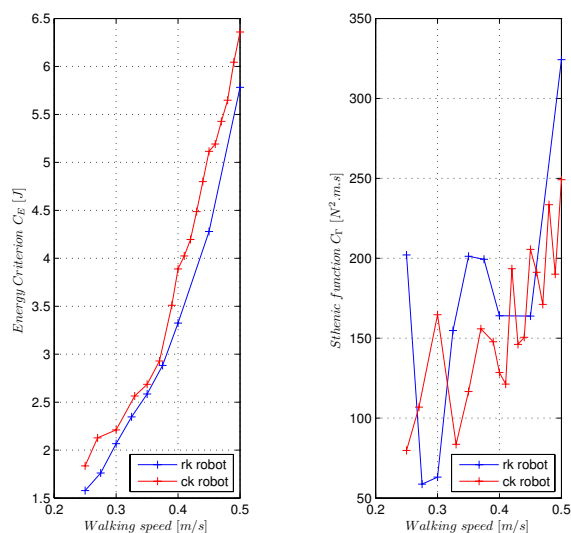
---

[1] http://www.lirmm.fr/~fraisse/R2A2/

REFERENCES

Banno, Y., Harata, Y., Taji, K., and Uno, Y. (2009). Optimal trajectory design for parametric excitation walking. In *2009 IEEE/RSJ International Conference on Intelligent Robots and Systems, IROS 2009*, 3202–3207.

Cabodevila, G. (1997). *Determination of energy optimal gaits of biped robots.* Phd thesis, University of Strasbourg, France. In french.

Cabodevila, G. and Abba, G. (1997). Quasi optimal gait for a biped robot using genetic algorithm. In *Proceedings of the IEEE International Conference on Systems, Man and Cybernetics*, volume 4, 3960–3965.

Chevallereau, C. and Aoustin, Y. (2001). Optimal reference trajectories for walking and running of a biped robot. *Robotica*, 19(5), 557–569.

Chevallereau, C., Bessonnet, G., Abba, G., and Aoustin, Y. (2009). *Bipedal robots: modeling, design and building walking robots.* ISTE and Wiley Editions, New York.

Collins, S., Wisse, M., and Ruina, A. (2001). A three-dimensional passive-dynamic walking robot with two legs and knees. *International Journal of Robotics Research*, 20(7), 607–615.

Fletcher, R. (1987). *Practical Method of Optimization.* John Wiley & Sons Ltd.

Hajek, B. (1988). Cooling schedules for optimal annealing. *Mathematic of Operation Research*, 13(2), 311–329.

Khalil, W. and Dombre, E. (2002). *Modeling, identification and control of robots.* Hermes Sciences Europe.

Lagarias, J., Reeds, J., Wright, M., and Wright, P. (1998). Convergence properties of the nelder-mead simplex method in low dimensions. *SIAM J. Optimization*, 9, 112–147.

McGeer, T. (1990). Passive dynamic walking. *Int. J. Rob. Research*, 9(2), 62–82.

Park, J. and Choi, M. (2004). Generation of an optimal gait trajectory for biped robots using a genetic algorithm. *JSME International Journal, Series C: Mechanical Systems, Machine Elements and Manufacturing*, 47(2), 715–721.

Plestan, F., Grizzle, J., Westervelt, E., and Abba, G. (2003). Stable walking of a 7-dof biped robot. *IEEE Transactions on Robotics and Automation*, 19(4), 653–668.

Roussel, L., de Wit, C.C., and Goswami, A. (1998). Generation of energy optimal complete gait cycles for biped robots. In *Proceedings - IEEE International Conference on Robotics and Automation*, volume 3, 2036–2041.

Sardain, P., Rostami, M., and Bessonnet, G. (1998). An anthropomorphic biped robot: Dynamic concepts and technological design. *IEEE Transactions on Systems, Man, and Cybernetics Part A:Systems and Humans.*, 28(6), 823–838.

Sardain, P., Rostami, M., Thomas, E., and Bessonnet, G. (1999). Biped robots: Correlations between technological design and dynamic behavior. *Control Engineering Practice*, 7(3), 401–411.

Scarfogliero, U., Folgheraiter, M., and Gini, G. (2004). Advanced steps in biped robotics: Innovative design and intuitive control through spring-damper actuator. In *2004 4th IEEE-RAS International Conference on Humanoid Robots*, volume 1, 196–214.

Fig. 7. Comparison of ground reaction forces for the walking speed to 0.3 m/s

Fig. 8. Evolution of optimal energy criterion versus walking speed (on the left). Evolution of the corresponding sthenic function (on the right).

HYDROÏD. In the future, an extension of this work with others set of orthogonal functions such as "Bézier" functions (in articular and in Cartesian coordinates) and the spline function in Cartesian coordinates will be considered. Another extension is to integrate the radii r_1 and r_2 in the parameter vector. For mechanical design, another shape of knee surface allows us to obtain an additional energetic profit.

Scarfogliero, U., Folgheraiter, M., and Gini, G. (2005). Larp, biped robotics conceived as human modeling. *Lecture Notes in Computer Science (including subseries Lecture Notes in Artificial Intelligence and Lecture Notes in Bioinformatics)*, 3575 LNAI, 299–314.

Scheint, M., Sobotka, M., and Buss, M. (2008). Compliance in gait synthesis: Effects on energy and gait. In *2008 8th IEEE-RAS International Conference on Humanoid Robots, Humanoids 2008*, 259–264.

Shafii, N., Aslani, S., Nezami, O., and Shiry, S. (2010). Evolution of biped walking using truncated fourier series and particle swarm optimization. *Lecture Notes in Computer Science (including subseries Lecture Notes in Artificial Intelligence and Lecture Notes in Bioinformatics)*, 5949 LNAI, 344–354.

Spong, M. and Vidyasagar, M. (1991). *Robot dynamics and control*. John Wiley & Sons, New-York.

Tlalolini, D., Chevallereau, C., and Aoustin, Y. (2009). Comparison of different gaits with rotation of the feet for a planar biped. *Robotics and Autonomous Systems*, 57(4), 371–383.

Tlalolini, R. (2008). *Génération de mouvements optimaux de marche pour des robots bipèdes 3D*. Phd thesis, University of Nantes, Nantes, France. In french.

Wu, T.Y. and Yeh, T.J. (2008). Optimal design and implementation of an energy-efficient, semi-active biped. In *Proceedings - IEEE International Conference on Robotics and Automation*, 1252–1257.

Appendix A. MATRIX EXPRESSION OF THE DYNAMIC MODEL

The mass-inertia matrix of the rolling knee robot defined by equation (19) has the following expression:

$$D(\mathbf{q}) = \tag{A.1}$$

$$\begin{pmatrix} d_{11} & 0 & d_{13} & d_{14} & 0 & 0 & 0 & d_{18} & d_{19} \\ 0 & d_{22} & 0 & 0 & d_{25} & d_{26} & 0 & d_{28} & d_{29} \\ d_{13} & 0 & d_{33} & d_{34} & 0 & 0 & 0 & d_{38} & d_{39} \\ d_{14} & 0 & d_{34} & d_{44} & 0 & 0 & 0 & d_{48} & d_{49} \\ 0 & d_{25} & 0 & 0 & d_{55} & d_{56} & 0 & d_{58} & d_{59} \\ 0 & d_{26} & 0 & 0 & d_{56} & d_{66} & 0 & d_{68} & d_{69} \\ 0 & 0 & 0 & 0 & 0 & 0 & d_{77} & d_{78} & d_{79} \\ d_{18} & d_{28} & d_{38} & d_{48} & d_{58} & d_{68} & d_{78} & d_{88} & 0 \\ d_{19} & d_{29} & d_{39} & d_{49} & d_{59} & d_{69} & d_{79} & 0 & d_{99} \end{pmatrix}$$

with $d_{11} = I_{p1} + m_{p1} s_{p1}{}^2$, $d_{13} = m_{p1} s_{p1} l_1' \cos\theta_1 + m_{p1} s_{p1} r_1 \cos\alpha_5$, $d_{14} = m_{p1} s_{p1} l_2' \cos(q_2 - q_{p1}) + m_{p1} s_{p1} r_2 \cos\alpha_5$, $d_{18} = m_{p1} s_{p1} \cos q_{p1}$,
$d_{19} = m_{p1} s_{p1} \sin q_{p1}$, $d_{22} = m_{p1} s_{p1}{}^2 + I_{p1}$,
$d_{25} = m_{p1} s_{p1} l_2' \cos(q_3 - q_{p2}) + m_{p1} s_{p1} r_2 \cos\alpha_6$,

$d_{26} = m_{p1} s_{p1} l_1' \cos(q_4 - q_{p2}) + m_{p1} s_{p1} r_1 \cos\alpha_6$,
$d_{28} = m_{p1} s_{p1} \cos q_{p2}$, $d_{29} = m_{p1} s_{p1} \sin q_{p2}$,
$d_{33} = I_1 + m_1 (s_1 - r_1)^2 + m_{p1} l_1'{}^2 + (m_1 + m_{p1}) r_1{}^2 + 2 m_1 (s_1 - r_1) r_1 \cos\alpha_2 + 2 m_{p1} l_1' r_1 \cos\alpha_2$,
$d_{34} = (m_1 + m_{p1}) r_1 r_2 - (m_1 + m_{p1}) r_1 l_2' \cos\theta_2 + (m_{p1} l_1 + m_1 s_1) l_2' \cos\theta_2 + (m_1 + m_{p1}) r_1 (l_2 - r_2) \cos\alpha_1 + (m_1 s_1 + m_{p1} l_1 - (m_1 + m_{p1}) r_1) r_2 \cos\alpha_2$,
$d_{38} = (m_1 (s_1 - r_1) + m_{p1} l_1') \cos q_1 + (m_{p1} + m_1) r_1 \cos\gamma_1$,
$d_{39} = (m_1 (s_1 - r_1) + m_{p1} l_1') \sin q_1 + (m_1 + m_{p1}) r_1 \sin\gamma_1$,
$d_{44} = I_2 + (m_1 + m_{p1}) r_2{}^2 + m_1 l_2'{}^2 + m_2 s_2{}^2 + m_{p1} l_2'{}^2 + 2 (m_1 + m_{p1}) l_2' r_2 \cos\alpha_1$,
$d_{48} = ((m_1 + m_{p1}) l_2' + m_2 s_2) \cos q_2 + (m_1 + m_{p1}) r_2 \cos\gamma_1$,
$d_{49} = ((m_1 + m_{p1}) l_2' + m_2 s_2) \sin q_2 + (m_1 + m_{p1}) r_2 \sin\gamma_1$,
$d_{55} = I_2 + m_1 l_2'{}^2 + m_{p1} l_2'{}^2 + m_1 r_2{}^2 + m_{p1} r_2{}^2 + m_2 s_2{}^2 + 2 m_1 l_2' r_2 \cos\alpha_3 + 2 m_{p1} l_2' r_2 \cos\alpha_3$,
$d_{56} = (m_1 + m_{p1}) r_1 r_2 + m_{p1} l_2' (l_1 - r_1) \cos\theta_5 + m_1 l_2' (s_1 - r_1) \cos\theta_5 + (m_1 + m_{p1}) l_2' r_1 \cos\alpha_3 + m_1 r_2 (s_1 - r_1) \cos\alpha_4 + m_{p1} r_2 l_1' \cos\alpha_4$,
$d_{58} = ((m_1 + m_{p1}) l_2' + m_2 s_2) \cos q_3 + (m_1 + m_{p1}) r_2 \cos\gamma_2$,
$d_{59} = ((m_1 + m_{p1}) l_2' + m_2 s_2) \sin q_3 + (m_1 + m_{p1}) r_2 \sin\gamma_2$,
$d_{66} = I_1 - 2 m_{p1} l_1 r_1 - 2 m_1 r_1 s_1 + 2 m_1 r_1{}^2 + m_1 s_1{}^2 + 2 m_{p1} r_1{}^2 + m_{p1} l_1{}^2 + 2 (m_1 (s_1 - r_1) + m_{p1} l_1') r_1 \cos\alpha_4$,
$d_{68} = (m_1 (s_1 - r_1) + m_{p1} l_1') \cos q_4 + (m_1 + m_{p1}) r_1 \cos\gamma_2$,
$d_{69} = (m_1 (s_1 - r_1) + m_{p1} l_1') \sin q_4 + (m_1 + m_{p1}) r_1 \sin\gamma_2$,
$d_{77} = I_5 + m_5 s_5{}^2$, $d_{78} = -m_5 s_5 \cos q_5$,
$d_{79} = -m_5 s_5 \sin q_5$, $d_{88} = m$, $d_{99} = m$.

with $\theta_1 = q_1 - q_{p1}$, $\theta_2 = q_1 - q_2$, $\theta_5 = q_4 - q_3$,
$\alpha_1 = \frac{r_1 \theta_2}{r_1 + r_2}$, $\alpha_2 = \frac{r_2 \theta_2}{r_1 + r_2}$, $\alpha_3 = \frac{r_1 (q_4 - q_3)}{r_1 + r_2}$, $\alpha_4 \frac{r_2 (\theta_5)}{r_1 + r_2}$,
$\alpha_5 = \frac{-q_{p1} r_1 - q_{p1} r_2 + r_1 q_1 + r_2 q_2}{r_1 + r_2}$,
$\alpha_6 = \frac{-q_{p2} r_1 - q_{p2} r_2 + r_1 q_4 + r_2 q_3}{r_1 + r_2}$.

Appendix B. MATRIX EXPRESSION OF THE IMPACT MODEL

The expression of the vector $\Delta_i \in \mathbb{R}^{9 \times 1}$ is:

$$\Delta_i = D^{-1} A_c^T I_R \tag{B.1}$$

$$\Delta_i = \begin{bmatrix} \Delta_0 \\ \Delta_1 \\ \Delta_2 \\ \Delta_3 \\ \Delta_3 \\ \Delta_5 \\ \Delta_6 \\ \Delta_x \\ \Delta_z \end{bmatrix} \tag{B.2}$$

The values Δ_1 to Δ_6 can then be directly used in the expression of the impact conditions given in 3.2.